

Type II Kinase Inhibitors Targeting Cys-Gatekeeper Kinases Display Orthogonality with Wild Type and Ala/Gly-Gatekeeper Kinases

Cory A. Ocasio,*†,‡,§,¶ Alexander A. Warkentin,‡,§ Patrick J. McIntyre,§ Krister J. Barkovich,‡
Clare Vesely,† John Spencer,|| Kevan M. Shokat,‡,§ and Richard Bayliss,‡,§

[†]Genome Damage and Stability Centre, School of Life Sciences, University of Sussex, Falmer, Brighton BN1 9RQ, U.K.

[‡]Howard Hughes Medical Institute and Department of Cellular and Molecular Pharmacology, University of California, San Francisco, 600 16th Street, San Francisco, California 94158-2280, United States

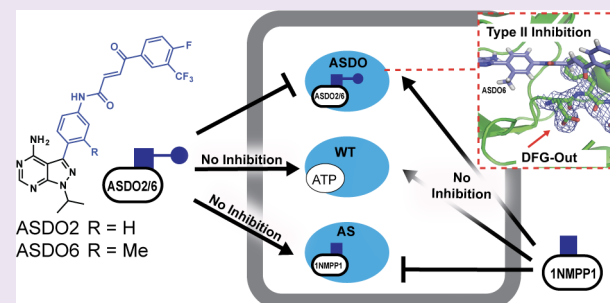
[§]Department of Molecular and Cell Biology, University of Leicester, Henry Wellcome Building, Leicester LE1 9HN, U.K.

^{||}Department of Chemistry, School of Life Sciences, University of Sussex, Falmer, Brighton BN1 9QJ, U.K.

[¶]School of Molecular and Cellular Biology, Faculty of Biological Sciences, University of Leeds, Leeds LS2 9JT, U.K.

Supporting Information

ABSTRACT: Analogue-sensitive (AS) kinases contain large to small mutations in the gatekeeper position rendering them susceptible to inhibition with bulky analogues of pyrazolopyrimidine-based Src kinase inhibitors (e.g., PP1). This “bump-hole” method has been utilized for at least 85 of ~520 kinases, but many kinases are intolerant to this approach. To expand the scope of AS kinase technology, we designed type II kinase inhibitors, ASDO2/6 (analogue-sensitive “DFG-out” kinase inhibitors 2 and 6), that target the “DFG-out” conformation of Cys-gatekeeper kinases with submicromolar potency. We validated this system *in vitro* against Greatwall kinase (GWL), Aurora-A kinase, and cyclin-dependent kinase-1 and in cells using M110C-GWL-expressing mouse embryonic fibroblasts. These Cys-gatekeeper kinases were sensitive to ASDO2/6 inhibition but not AS kinase inhibitor 3MB-PP1 and vice versa. These compounds, with AS kinase inhibitors, have the potential to inhibit multiple AS kinases independently with applications in systems level and translational kinase research as well as the rational design of type II kinase inhibitors targeting endogenous kinases.



OVERVIEW OF KINASES AND ANALOGUE-SENSITIVE KINASE TECHNOLOGY

Eukaryotic protein kinases represent one of the largest protein families in the human genome with ~520 members and constitute ~2% of all human genes.¹ These enzymes catalyze the transfer of the γ -phosphate group from ATP to serine (Ser), threonine (Thr), or tyrosine residues on their substrate proteins or peptides. This post-translational modification is a critical and nearly ubiquitous mode of intracellular signaling, with ~30% of all proteins being phosphorylated.^{2,3} It is, therefore, no surprise that aberrant expression and activation of this class of proteins often lead to a variety of diseases with ~244 kinases mapping to disease loci and cancer amplicons.^{1,4,5}

One way to study kinase function and manage dysregulated kinases is through development of selective kinase inhibitors; however, because of the high degree of structural similarity, particularly in and around the ATP-binding pocket, it is often difficult to target an individual kinase with small-molecule inhibitors. One way to circumvent this issue is by employing a chemical–genetic strategy that takes advantage of a structurally conserved, mostly hydrophobic residue within the kinase active site, termed the gatekeeper residue.^{6–8} Mutation of this residue

from a normally bulky residue to a smaller one, such as alanine (Ala) or glycine (Gly), engenders an analogue-sensitive (AS) kinase containing a unique binding site that can be exploited pharmacologically with bulky ATP analogues such as 1NMPPI,⁸ 3MB-PP1,⁸ and the recently developed staralogs⁷ (Figure 1A–D). This “bump-hole” method has been utilized for the study of at least 85 different kinases, yet despite this level of success, there are still a number of kinases, coined “intolerant” kinases, that do not tolerate gatekeeper mutations.^{8–11} To expand the scope of AS technology, researchers have identified second-site mutations or suppressor of Gly-gatekeeper mutations (*sogg*) that restore the kinase activity to some “intolerant” AS kinases (applied to at least 11 kinases so far) when the gatekeeper is Gly or Ala.^{8,10} In addition, electrophile-sensitive (ES) kinases can be selectively inhibited by electrophilic, bulky PP1 or ATP analogues (Figure 1E) [e.g., fluoromethylketobenzyl (FMKB)-PP1, acrylamido-anilinoquinazolines (AQZ), and 5'-vinylsulfonyl adenosine (VSA)] by targeting cysteine (Cys) mutations within the gatekeeper or

Received: June 26, 2018

Accepted: September 21, 2018

Published: September 21, 2018

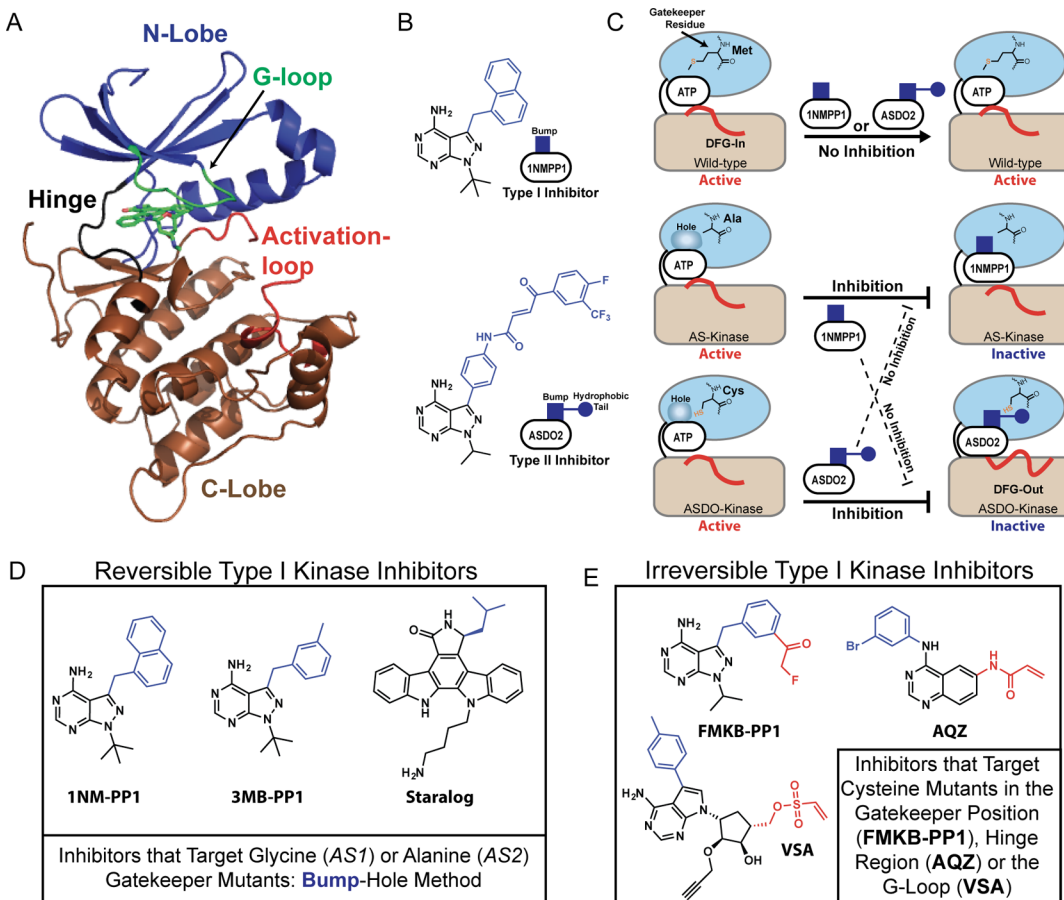


Figure 1. AS and ASDO kinase systems. (A) Tertiary structure of the staurosporine-bound GWL domain with key features highlighted (Protein Data Bank entry 5LOH). (B) Chemical structures of 1NM-PP1 and ASDO2. (C) Cartoon depicting a wild type kinase (top) with a bulky methionine-gatekeeper residue. Mutating the gatekeeper residue to a smaller alanine (or glycine) residue generates an AS kinase (middle). Mutating the gatekeeper residue to a cysteine generates an AS kinase that is susceptible to inhibition by novel “DFG-out” conformation-targeting inhibitors (ASDOs; ASDO2 depicted here, bottom). The AS and ASDO kinase systems are orthogonal to wild type kinases and each other. (D) Panel of reversible type I inhibitors that target alanine- or glycine-gatekeeper mutants. (E) Panel of irreversible type I inhibitors that target cysteine mutations in the gatekeeper, hinge region, or G-loop regions. Structural features highlighted in blue complement the expanded hydrophobic pocket that is generated by mutation of the gatekeeper residue to alanine or glycine, and features highlighted in red represent cysteine-reactive, electrophilic warheads (fluoromethylketone, acrylamide, and vinylsulfone).

other positions vicinal to the ATP-binding pocket [i.e., in the Gly-rich loop (G-loop) or hinge region (Figure 1A)].^{9,12–18} However, these approaches appear to be highly specific to individual kinases and not widely applicable. This also limits the possibility of differentially inhibiting two kinases with two orthogonal chemical–genetic systems. Such a dual bio-orthogonal approach would be ideal for investigating kinase signaling crosstalk, synthetic lethality, and many other areas of systems biology and translational research across a diverse set of kinase drug targets.

In this study, we report the development of a new chemical–genetic approach based on a Cys-gatekeeper mutation and noncovalent, type II mode of kinase inhibition that targets the inactive “DFG-out” kinase conformation (Figure 1C).¹⁹ We verified this approach with three divergent Ser/Thr kinases: Greatwall kinase (GWL), Aurora-A kinase (AAK), and cyclin-dependent kinase-1 (Cdk1). To demonstrate compound efficacy in cells, we measured phosphorylation of the physiologic GWL substrate α -endosulfine (ENSA)²⁰ and cellular proliferation, a phenotype functionally linked to GWL activity,^{21,22} in wild type (WT)- and M110C (MC) GWL-expressing mouse embryonic fibroblasts (MEFs).

ASDO2 (analogue-sensitive “DFG-out” kinase inhibitor 2) specifically inhibited production of phospho-ENSA (pENSA) and attenuated proliferation in MC-GWL-expressing MEFs but not in WT-GWL-expressing cells. Together, these data support expanding the AS kinase inhibitor tool set with “DFG-out” targeting ASDO inhibitors, which in combination with established AS kinase inhibitors would allow for the independent targeting of at least two distinct kinases (Figure 1C).

RESULTS AND DISCUSSION

Approaches Utilized To Expand Analogue-Sensitive Kinase Technology. The starting point of this study was an effort to develop an AS version of microtubule-associated Ser/Thr kinase-like (MASTL) protein, commonly known as GWL, to investigate its mitotic functions and role in the cell cycle.²³ Overexpression and immunoprecipitation of FLAG-tagged GWL constructs provided a means to assess the activity of a cohort of GWL mutants (Figure 2A). This assay demonstrated that GWL is an “intolerant” kinase evidenced by the inactivity of the AS1 (M110G) and AS2 (M110A) GWL kinase alleles (Figure 2B,C and Figure S1A), and neither *sogg* mutations nor

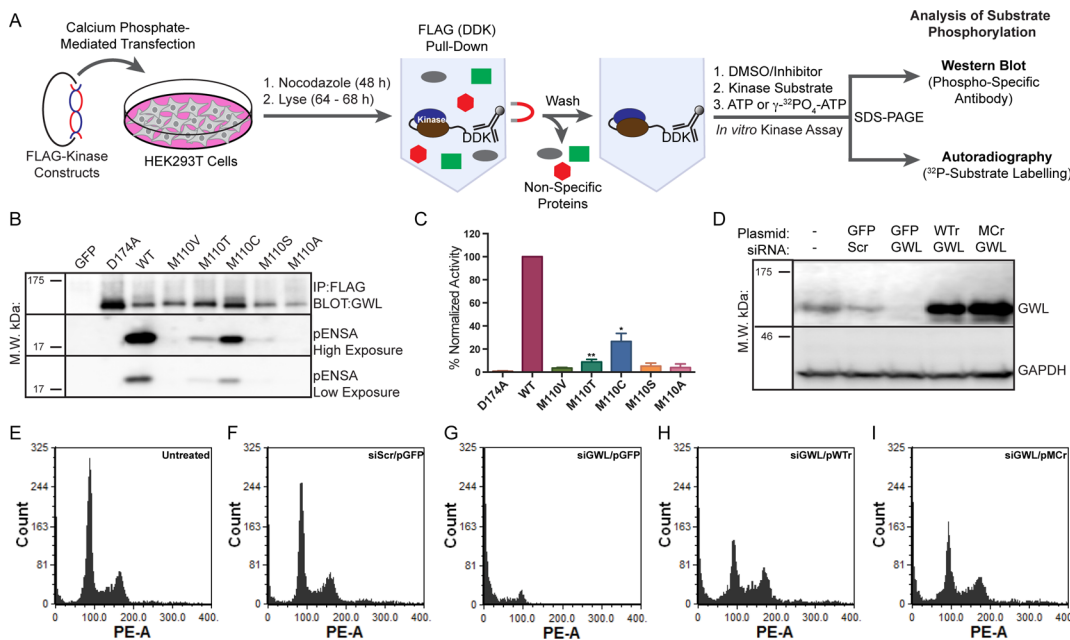


Figure 2. Systematic mutational analysis of the GWL-gatekeeper position. (A) General workflow for the immunoprecipitation-mediated kinase assay. (B and C) Systematic analysis of gatekeeper mutations in the GWL ATP-binding pocket. (D) Rescue of RNAi-mediated GWL depletion by co-expression with siRNA-resistant WT- and MC-GWL constructs (pWTr and pMCr, respectively). (E–I) FACS cell cycle analysis of HeLa cells. Kinase assays were performed at least three times per mutation; quantitation using ImageJ (version 1.47) (densitometry) of the average normalized percent kinase activity (pENSA:GWL ratio used as a readout of kinase activity) \pm the standard deviation was performed using Prism 6.0, and the results were plotted using Prism 6.0. The *t*-test statistical module of Prism 6.0 was used to determine *p*-values for D174A versus M110C and M110T (*: $P \leq 0.05$; **: $P \leq 0.01$).

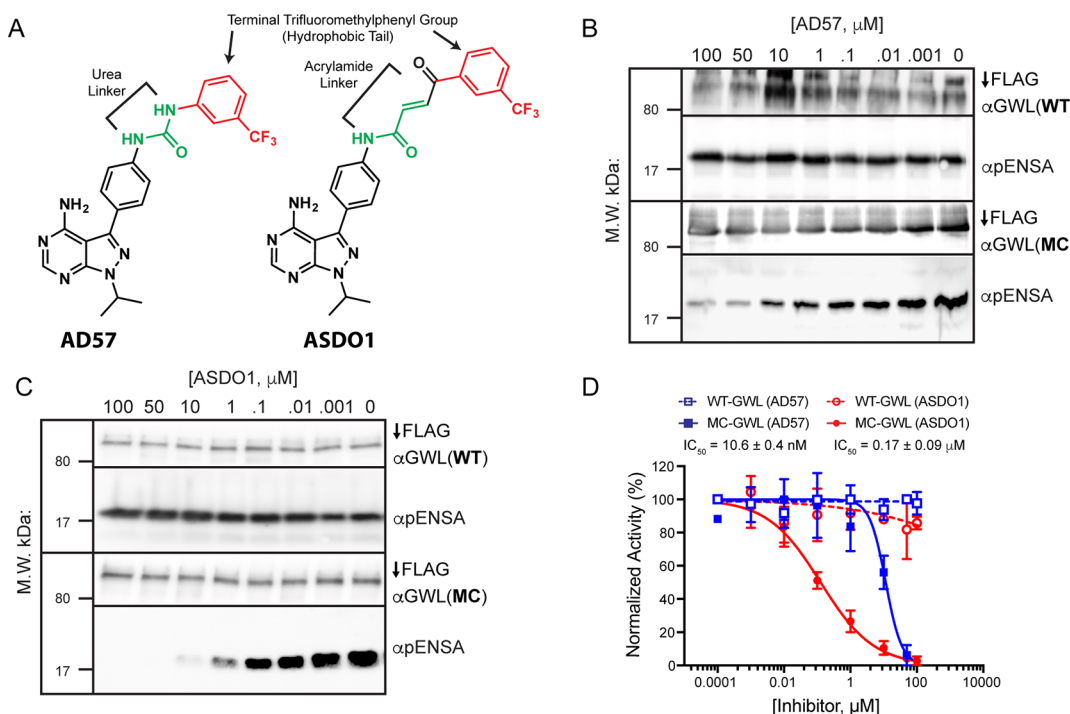


Figure 3. Establishing the inhibitory activity of AD57 and ASDO1 in the GWL kinase assay. (A) Chemical structures of AD57 and ASDO1. Structural features highlighted in green are linkers that bridge the PP1 moiety with the terminal trifluoromethylphenyl (red) group. (B and C) FLAG-tagged WT- and MC-GWL kinase assays in the presence of increasing concentrations of AD57 and ASDO1, respectively. (D) Kinase activity was quantified using ImageJ (version 1.47) (densitometry) and reported as the average normalized percent kinase activity \pm the standard deviation.

the ES kinase approach was capable of generating an AS-GWL system (Figure S1A–G). In the first instance, we decided to introduce *sogg* mutations at the analogous positions in GWL,

which included mutations that were previously successful for kinases such as Pto (L68I), APH(3')-IIIa (N268T), and GRK2 (S268V) (Figure S1G).¹⁰ Only one of these mutations,

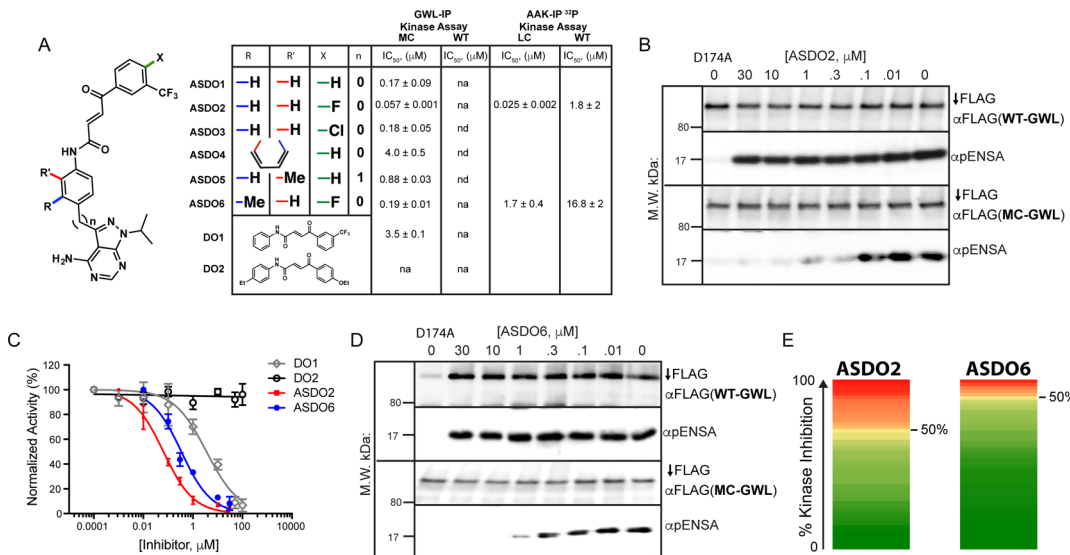


Figure 4. *In vitro* analysis of ASDO derivatives. (A) The potency of synthetic AD57 derivatives (ASDOs), DO1, and commercially available DO2 was assessed using an *in vitro* immunoprecipitation kinase assay. na, not applicable; nd, not determined. The potencies of ASDO2 (B and C) and ASDO6 (C and D) were determined using FLAG-tagged WT- and MC-GWL kinase assays. (E) ASDO2 and ASDO6 were screened at 1 μM against a panel of 50 kinases, carefully selected to represent the kinome, using the Kinase Express Screen (International Centre for Kinase Profiling, University of Dundee, Dundee, U.K.).

V61I-GWL, augmented GWL activity, evidenced by an increased level of myelin basic protein phosphorylation, but did not restore activity of the double mutant V61I/M110A-GWL (Figure S1B). Bioinformatically, we identified sites in the G-loop consensus sequence (GxGxxG) that deviated from those of other AGC kinases, but reversion mutations in the G-loop, made to adopt the more common amino acids, had a meager (S42G) to no (S42G/A45S) effect in combination with M110A-GWL (Figure S1A,C).²⁴

Initial efforts to identify *sogg* mutations for Ala-gatekeeper GWL were unsuccessful, and thus, we hypothesized that other small amino acids, presumably preserving an expanded hydrophobic ATP-binding pocket, might be useful in combination with previously identified or new *sogg* mutations. To explore this idea further, the gatekeeper position was scanned with relatively small amino acids, which led to the discovery that the level of MC-GWL-mediated phosphorylation of ENSA was only 4-fold lower than that of the WT (Figure 2B,C). Furthermore, through FACS analysis, we showed that RNAi-resistant MC-GWL, unlike M110A-GWL, was able to restore G₁, S, and G₂/M cellular levels to the same extent as an siRNA-resistant WT rescuing plasmid in GWL-depleted HeLa cells (Figure 2D–I and Figure S2A–F). This result inspired the generation of an ES kinase system; however, the electrophilic inhibitors AG1-2 and FMKB-PP1 (Figure 1E and Figures S1D,E and S2), which were validated against T338C-c-Src, did not robustly inhibit MC-GWL at concentrations of 20 μM (Figure S1D,E).⁹ Of the other small gatekeeper mutations, M110T-GWL displayed ~8% activity compared to that of the WT, and thus, we introduced Cys mutations into an M110T-GWL mutant to mimic the cysteines in the hinge regions of EphB3 (C717) and EGFR (C797), M110T/G116C and M110T/D117C.^{13,15} In combination with a Thr gatekeeper, similar mutations in EphB1 (G703C) and c-Src (S345C), to name a few, can be targeted using electrophilic quinazoline-based inhibitors [e.g., AQZ (Figure 1D)], but because of the inactivity of these GWL double mutants, we were not able to apply them (Figure S1F,G).^{13,15}

AD57 Analogues Specifically Target MC-GWL *In Vitro*.

Because of the inefficacy of known ES kinase inhibitors against MC-GWL, we decided to generate novel inhibitors based on the structure of AD57²⁵ (Figure 3A and Figure S3). We surmised that replacement of the urea linker with an acrylamide linker might allow selective targeting by a nucleophilic Cys mutant.¹⁶ AD57 also seemed like an ideal candidate as it selectively inhibited MC-GWL with a modest IC₅₀ value of 10.6 ± 0.4 μM and displayed no inhibitory activity against WT-GWL (Figure 3B,D). ASDO1, the first in a series of AD57 analogues, was synthesized by coupling of an anilinopyrazolopyrimidine with a 3-benzoylacrylic acid chloride (Supplementary Schemes 1–3 and Figure 4A).^{9,26} The resulting compound contained an acrylamide linker bridging the pyrazolopyrimidine moiety with a trifluoromethylbenzoyl group. This feature is similar to a *m*-trifluoromethylphenyl group, which is commonly incorporated into some type II kinase inhibitors.^{19,27} ASDO1 (analogue-sensitive “DFG-out” kinase inhibitor 1) (Figure 3A) completely abrogated MC-GWL activity at a concentration of 20 μM without inhibiting WT-GWL (Figure S3). By assaying AD57 and ASDO1 more rigorously using the immunoprecipitation-based kinase assay with ENSA as the substrate, we were able to show that ASDO1 exhibited a >60-fold improvement in potency against MC-GWL with an IC₅₀ value of 0.17 ± 0.09 μM and remained exquisitely selective for MC-GWL versus WT-GWL even up to concentrations as high as 100 μM (Figures 3C,D and 4A and Figure S4A,B).

Structural studies using an AD57-c-Src co-crystal structure predicted that formal halogenation of the terminal phenyl ring with *o*-fluorine and *p*-chlorine substituents would fine-tune the selectivity profile of AD57. Indeed, these halogenated AD57 derivatives maintained inhibitory activity toward Ret, Raf, Src, and S6K, reduced the level of mTor inhibition, and led to significantly less toxicity in a multiple-endocrine neoplasia type 2 *Drosophila* model system.²⁵ In an attempt to fine-tune the selectivity of ASDO1 toward MC-GWL versus WT-GWL, we synthesized halogenated and bulkier, nonhalogenated ASDO

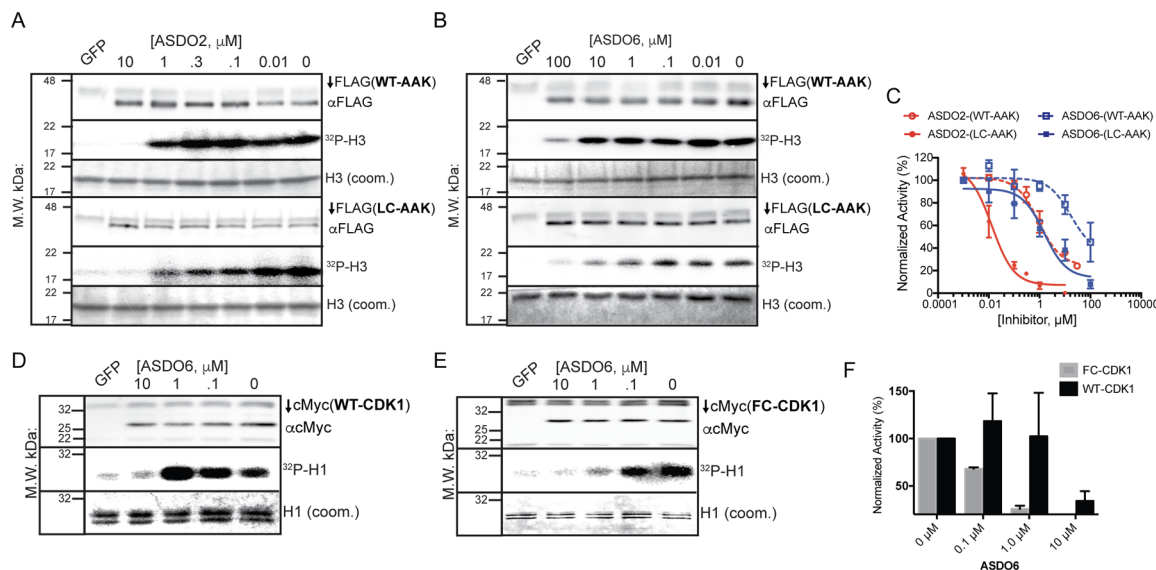


Figure 5. *In vitro* analysis of **ASDO2** and **ASDO6** in FLAG-AAK and Myc-Cdk1 kinase assays. The inhibitory activity of **ASDO2** (A and C) and **ASDO6** (B and C) against FLAG-tagged WT- and LC-AAK constructs was assessed using a radioactive kinase assay to detect the $^{32}\text{PO}_4\text{-H3}$ substrate. (D and E) The inhibitory activity of **ASDO6** against MYC-tagged WT and F80C-Cdk1 was assessed using a radioactive kinase assay for the detection of the $^{32}\text{PO}_4\text{-H1}$ substrate. (C and F) Kinase activity was quantified using ImageJ (version 1.47) (densitometry) and reported as the average normalized percent kinase activity \pm the standard deviation.

derivatives by first incorporating acetophenones into the microwave-assisted aldol condensation with glyoxylic acid to yield 3-benzoylacrylic acids,²⁶ which after conversion to acid chlorides were later coupled with anilinopyrazolopyrimidines (*Supplemental Schemes 2 and 3* and *Figure 4A*) to produce **ASDO2–6**.

ASDO2 contains a trifluoromethylbenzoyl group with a *p*-fluoro substituent and demonstrated an ~3-fold improvement in potency, whereas the effect of the *p*-chloro substitution (**ASDO3**) was negligible (*Figure 4A–C* and *Figure S4C–E*). We also explored the activity of bulkier derivatives in the hope of improving their selectivity for Cys-gatekeeper versus WT kinases. Unfortunately, replacing the central benzene ring with a naphthyl group [**ASDO4** (*Figure 4A* and *Figure S4F*)] or a 3-methylbenzyl group [**ASDO5** (*Figure 4A* and *Figure S4G*)] dramatically weakened inhibitory activity; however, the 2-methylphenyl substitution of the inner benzene ring (**ASDO6**) in combination with the *p*-fluoro substitution seen in **ASDO2** resulted in a compound with inhibitory activity almost equal to that of the **ASDO1** precursor (*Figure 4A,C,D* and *Figure S4H,I*). Interestingly, **DO1**, which lacks the pyrazolopyrimidine group, also displayed monospecific targeting of MC-GWL versus WT-GWL but with attenuated inhibitory activity compared to that of **ASDO1** (*Figure 4A,C* and *Figure S4J,K*), suggesting that the selectivity filter resulting in Cys-gatekeeper kinase specificity lies within the phenylbenzoylacrylamide scaffold and that the electrophilic olefin might be targeted by the Cys-gatekeeper residue. Furthermore, replacement of the trifluoromethyl group of **DO1** with a *p*-ethoxy substituent (**DO2**) completely ablated inhibitory activity toward both WT-GWL and MC-GWL (*Figure 4A,C* and *Figure S4L,M*). Interestingly, some type II kinase inhibitors (e.g., **AD57** and **Sorafenib**^{25,27}) possess a trifluoromethyl substituent on their terminal phenyl ring, which occupies space in an allosteric hydrophobic pocket unique to the inactive kinase conformation.^{19,28} In contrast to the case of **DO1**, the lack of inhibitory activity of **DO2** hints at the possibility that

this series of compounds, like the parent compound **AD57**, might stabilize the inactive “DFG-out” kinase conformation.

To establish the importance of the bulkier central ring of **ASDO6**, both **ASDO2** and **ASDO6** were subjected to a rigorous kinase inhibition profiling screen (International Centre for Kinase Profiling, University of Dundee, Kinase Profiling Express Screen). At 1 μM , **ASDO2** inhibited 15 of 50 kinases with $\geq 60\%$ inhibitory activity (60–95%); however, as is the case with classical AS kinase inhibitors, the increased bulk of the central benzene ring of **ASDO6** likely accounts for the decrease in the number of WT kinases targeted with $>60\%$ inhibitory activity (62–84%) (only four of 50 kinases). Note that the higher end of the inhibitory range decreased from 95% for **ASDO2** to 84% for **ASDO6**, providing further evidence that the bulkier **ASDO6** derivative is more refractory toward WT kinases (*Figure 4E* and *Figure S5A,B*).

ASDO6 Targets AAK and Cdk1 Bearing a Cys Gatekeeper. Next, we sought to place ASDO compounds within the pantheon of general AS kinase inhibitors. To do this, we mutated the gatekeeper positions of AAK (L210) and *Xenopus laevis* Cdk1 (F80) to cysteines and subjected them to kinase assays with increasing concentrations of **ASDO2** or **ASDO6** (*Figure 5A–F* and *Figure S6A–C*). Both kinases tolerated the Cys-gatekeeper mutation with improved kinase activity (Cdk1) or a slight decrease in kinase activity (AAK) compared to that of the WT (*Figure S6B,C*). Moreover, **ASDO2** inhibited L210C (LC)-AAK with the greatest potency, demonstrating an IC_{50} value of $25 \pm 2 \text{ nM}$ (*Figures 4A* and *5A,C*), and was >70 -fold selective in targeting LC-AAK versus WT-AAK. Although less potent than **ASDO2** inhibition, **ASDO6** inhibition of LC-AAK ($\text{IC}_{50} = 1.7 \pm 0.4 \mu\text{M}$) and F80C-Cdk1 was ~ 10 -fold more selective than versus their WT counterparts (*Figure 5B–F*).

ASDO2 Selectively Inhibits MC-GWL in Cells. Although **ASDO6** inhibited fewer WT kinases with $>60\%$ inhibitory activity (*Figure 4E*), **ASDO2** displayed greater potency and specificity in GWL and AAK kinase assays (*Figure 4A*). We,

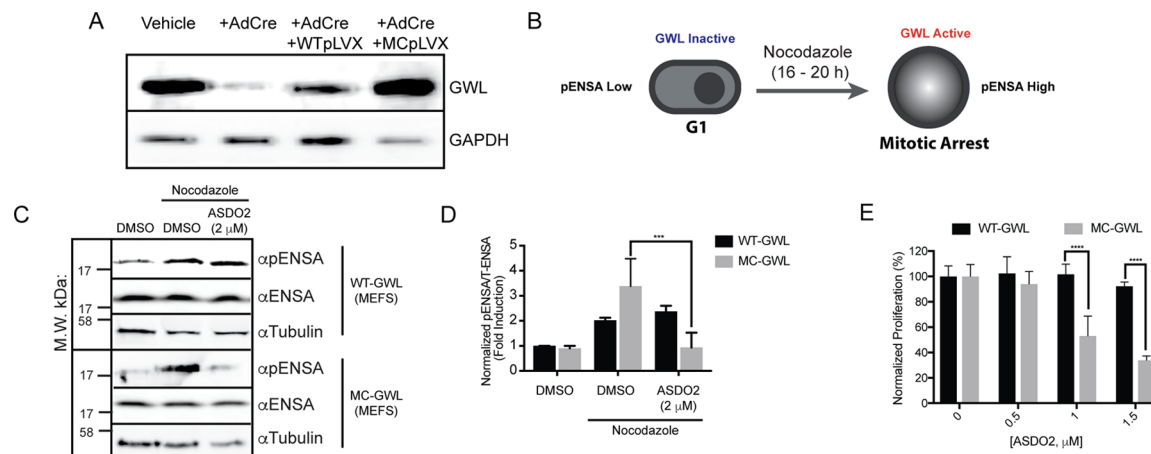


Figure 6. Cellular analysis of ASDO2 in WT- and MC-GWL-expressing mouse embryonic fibroblasts (MEFs). (A) Expression of exogenous WT- and MC-GWL confirmed by Western blot analysis. (B) Strategy used to fully activate GWL in MEFs. Cells were treated with 200 ng/mL nocodazole for 16–20 h before being harvested for downstream applications. (C and D) Mitotic cells were treated with 2 μM ASDO2 or DMSO for 4 h. ENSA, phospho-ENSA, and tubulin levels in cell lysates were determined by Western blot analysis. All experiments were repeated thrice, and activity (pENSA:ENSA ratio) was quantified using ImageJ (version 1.47) (densitometry), normalized to the DMSO control, and reported as the average fold induction relative to the DMSO control (without nocodazole) ± the standard deviation. (E) CellTiter Blue proliferation assays.

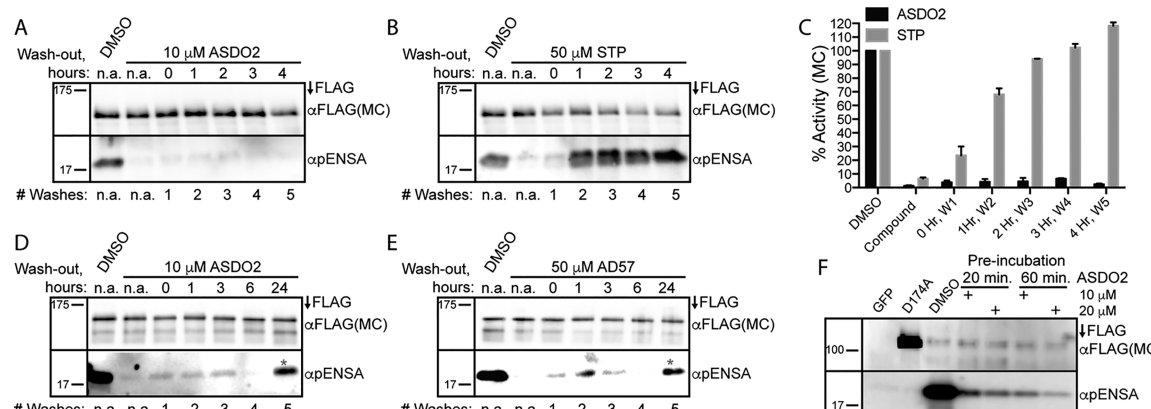


Figure 7. Comparison of the kinetics of binding of ASDO2 to kinase inhibitors staurosporine (STP, type I) and AD57 (type II). FLAG-tagged MC-GWL was treated with DMSO (A–F), ASDO2 (A, C, and D), STP (B and C), or AD57 (E) for 20 min and then subjected to GWL kinase assay conditions. These beads were also subjected to several washes (buffer exchange) for the indicated amount of time before the start of the kinase assay. (F) Kinase assays were performed with FLAG-tagged MC-GWL, preincubated with DMSO or ASDO2 for 20 or 60 min before the start of the kinase reaction. The reaction was started via addition of ATP and ENSA. All experiments were repeated thrice, and the average pENSA/FLAG(M110C-GWL) ratio was quantified using ImageJ (version 1.47) (densitometry) and normalized to the DMSO control (C).

therefore, opted to assess the effects of ASDO2 on cellular ENSA phosphorylation and proliferation in MEFs over-expressing WT- or MC-GWL. To establish cellular models for MC-GWL, we decided to employ MEFs containing loxP sites flanking exon 4 of the murine GWL gene.²⁹ Treatment of these cells with Cre-expressing adenovirus depleted GWL and allowed for reintroduction of human WT- or MC-GWL cDNA via lentiviral transduction (Figure 6A). After the presence of human GWL had been confirmed by Western blot analysis, both populations of WT- and MC-GWL-expressing cells were treated with nocodazole (200 ng mL⁻¹) for 16–20 h (Figure 6B). The activity of mitotic kinases increases substantially during mitosis, making the nocodazole-mediated mitotic arrest (M-arrest) essential for visualizing the cellular inhibition of ENSA phosphorylation; inhibition of an inactive kinase would reveal only background level phosphorylation. After M-arrest and treatment with 2 μM ASDO2 or dimethyl sulfoxide (DMSO) for 4 h, cells were harvested, lysed, and probed with

an anti-pENSA antibody by Western blot analysis, revealing monospecific inhibition of MC-GWL-mediated ENSA phosphorylation (Figure 6C,D). Functionally, GWL has been linked to cellular proliferation in several studies and thus serves as an ideal gauge for GWL activity.^{21,22} After growth in the presence of an inhibitor or DMSO for 5 days, we observed that only cells depleted of endogenous WT-GWL and over-expressing MC-GWL had dramatically reduced levels of proliferation in an ASDO2 concentration-dependent manner, thus confirming the utility of ASDO2 and possibly other ASDO derivatives in cellular models (Figure 6E).

ASDO2 Displays Relatively Slow-On/Slow-Off Binding/Dissociation Kinetics. At this point, it was still unclear how ASDO2 and ASDO6 monospecifically targeted MC-GWL versus WT-GWL (i.e., as a type I or II inhibitor), and the presence of an electrophilic, doubly activated olefin calls into question whether it interacts with MC-GWL in a reversible or irreversible manner. To further probe the mechanism of action

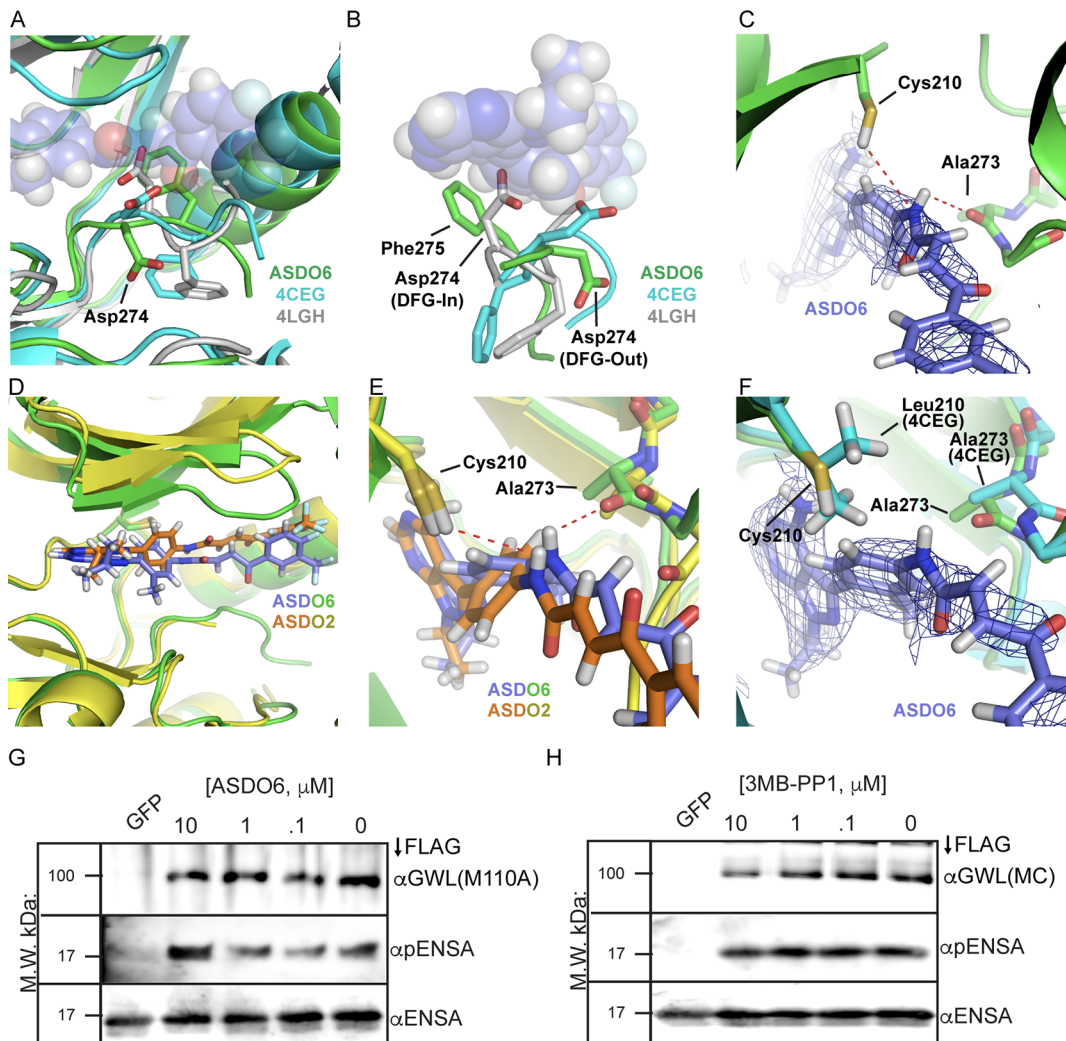


Figure 8. X-ray co-crystal structures of ASDO2 and ASDO6 with LC Aurora-A kinase. (A) Alignment of ASDO6-bound (PDB entry 6HJJ), ADP-bound (PDB entry 4CEG), and 1NM-PP1-bound (PDB entry 4LGH) structures reveals the orientation of their respective catalytic motif aspartic residues. (B) Close-up of panel A. (C) ASDO6 abuts the gatekeeper cysteine residue forming a weak electrostatic interaction with the thiol hydrogen of cysteine and a stronger hydrogen bonding interaction with the backbone of Ala273, serving to clamp ASDO6 within the nucleotide-binding site proximal to the gatekeeper position. (D) Comparison of the ASDO2- and ASDO6-bound LC-AAK structures. (E) Close-up of panel D. (F) Superimposition of the ASDO6- and ADP-bound structures reveals a potential conflict between the ASDO6-amide and the hydrophobic L210-gatekeeper residue. (G) ASDO6 and (H) 3MB-PP1 inhibitory activity was assessed against M110A-GWL and MC-GWL, respectively, using the immunoprecipitation kinase assay.

of ASDO2, we investigated the reversibility of inhibition in comparison to that of a type I inhibitor (staurosporine) and that of the parent type II inhibitor ADS7; note that type I inhibitors generally display fast-on/fast-off binding/dissociation kinetics, whereas type II inhibitors generally display slow-on/slow-off binding/dissociation kinetics.^{28,30}

Initially, a washout experiment with MC-GWL supported the notion of an ES kinase model system. Evidence for this is seen by the failure of ASDO2-treated (10 μM) MC-GWL to regain activity after five washes over a 4 h period compared to the quick reactivation of staurosporine (STP)-treated (50 μM) MC-GWL under the same conditions (Figure 7A–C). However, when we probed reactivation of MC-GWL after longer periods of time following washout of ASDO2 and ADS7 (bona fide type II inhibitor), it became evident that MC-GWL regained activity over time, but this reactivation took longer due to a relatively slower off-rate (Figure 7D,E). Importantly, activity may not have rebounded to levels demonstrated by

fully active MC-GWL (not treated with inhibitor) due to decomposition or destabilization of the protein over a 24 h period at 4 °C. Additionally, ASDO2 rapidly inhibited MC-GWL activity but with a slight difference in inhibitory activity between 20 and 60 min compound preincubation periods (Figure 7F). Taken together, these data suggest that ASDO2 shares similar slow-on/slow-off binding/dissociation kinetics with the type II inhibitor ADS7 but could also be acting, to a small extent, in an irreversible manner as inhibition marginally improves over time (Figure 7F). Unfortunately, expression, purification, and X-ray crystallography of full-length GWL have proven to be major technical challenges; therefore, to pin down the exact binding mode of ASDOs in GWL, technical innovations in GWL structural biology are required.²¹

ASDO2 and ASDO6 Demonstrate a Type II Inhibitor Binding Mode with LC-AAK. To cement the binding mode of ASDO2 and ASDO6, we determined the X-ray co-crystal structures with LC-AAK: ASDO2 [Protein Data Bank (PDB)

entry 6HJK] and **ASDO6** (PDB entry 6HJJ).³¹ Both compounds were sandwiched between the N- and C-terminal lobes bound to the ATP-binding pocket, making the expected interactions with the backbone of the hinge region (Glu211 and Ala213) and stretching all the way to the $\text{C}\alpha$ -helix, displacing it in comparison to the WT-AAK ADP-bound structure [PDB entry 4CEG (Figure S7A–D)]. In both cases, the DFG motif adopts an “out” conformation (DFG-out), in which Phe275 points into the ATP-binding pocket, while the terminal aromatic groups of both compounds are buried in a hydrophobic pocket adjacent to the $\text{C}\alpha$ -helix, indicative of type II kinase inhibitors (Figure 8A,B and Figure S7D).¹⁹ In fact, an overlay of the Asp274 residues of the 1NM-PP1-bound (type I, PDB entry 4LGH) and **ASDO2/6**-bound (type II) structures illustrates another key difference between type I and II inhibitors. The Asp residue flips 180° going from an active (Asp points into the ATP-binding pocket) to an inactive (Asp points outside of the ATP-binding pocket) conformation, allowing Phe to pack against **ASDO6** (Figure 8A,B and Figure S7D).¹⁹

In the **ASDO6**-bound structure, Cys210 appears to form a weak, electrostatic interaction with the amide “N”, and the Ala273 backbone carbonyl forms a strong hydrogen bond with the same amide group, serving as a molecular clamp that also brings to light the importance of the cysteine residue (Figure 8C). Comparing the **ASDO2**- and **ASDO6**-bound structures also sheds light on the molecular level basis for the decrease in the level of WT kinase targeting by **ASDO6**; **ASDO6** prefers binding to AAK only when the gatekeeper residue is a polar amino acid such as cysteine. Alignment of these structures shows that the methylphenyl ring of **ASDO6** twists in the direction of Cys210, bringing the amide closer to the Ala273 backbone; however, a water molecule fills the gap among **ASDO2**, Cys210, and the Ala273 backbone with all three elements forming a hydrogen bonding network in the **ASDO2**-bound structure (Figure 8D,E and Figure S7E).

As a result of placing the polar amide group of **ASDO6** closer to the gatekeeper residue, WT AAK, which harbors a hydrophobic Leu210-gatekeeper residue, would disfavor and destabilize the **ASDO6**-bound conformation (Figure 8F). On the basis of this hypothesis, other hydrophobic amino acids such as Ala should also attenuate **ASDO6** inhibitory activity, and replacing cysteine with a less polar amino acid or with Gly, which lacks a side chain, should abolish the molecular clamp mechanism and abrogate the **ASDO6**–GWL interaction. To test these hypotheses, we overexpressed, immunoprecipitated, and treated FLAG-M110A-GWL with **ASDO6** at concentrations of $\leq 10 \mu\text{M}$. As predicted, **ASDO6** was not able to inhibit M110A-GWL, nor was 3MB-PP1 able to inhibit M110C-GWL *in vitro* (Figure 8G,H), suggesting the two systems work independently of each other and could be used to differentially inhibit other combinations of kinases based on gatekeeper mutations to either cysteine or Ala/Gly.

■ DISCUSSION AND CONCLUSIONS

AS kinase technology has been employed to dissect the cellular functions of individual kinases across the kinase family, but there are still a number of kinases that remain averse to this methodology. To apply AS kinase technology, mutations that engender sensitivity to pharmacologic inhibition must also maintain sufficient kinase activity so that the mutant kinase can recapitulate WT cellular function. There are many ways to broaden the scope of AS kinase technology such as making sugg

mutations that rescues the activity of “intolerant” kinases when an Ala/Gly-gatekeeper mutation is present.¹⁰ Also, over the years, a number of different AS and ES systems that incorporate amino acids other than Ala or Gly, e.g., Cys or Thr,^{9,13,17,18} into the gatekeeper position have been developed; however, so far, these systems have not been widely utilized in the field, though some are still in their infancy. In terms of AS systems that have proven to be fruitful, a number of new reagents such as staralogs⁷ offer even greater specificity and potency, but to expand the scope of AS kinase technology further, we need not focus solely on engineering inhibitors against the active kinase conformation but take full advantage of all modes of pharmacologic inhibition. To date, type II inhibitors have been ignored when it comes to the development of chemogenomic technology, but this study is the first to provide an example of a chemical–genetic system based on Cys mutant kinase inhibition with a type II inhibitor, a system that we now call the **ASDO** (analogue-sensitive “DFG-out”) kinase system (Figure 1B,C).

Furthermore, type I and II kinase inhibitors bind to disparate kinase conformations, resulting in their catalytic inactivation.^{19,27,28} Because of evolutionary pressure to preserve the catalytically active kinase conformation, type I inhibitors encounter a very similar ATP-binding pocket across the kinome, made exploitable through the “bump-hole” method. The inactive kinase conformation is not bound by this evolutionary pressure and is more varied,²⁸ which may have hampered previous attempts to generate a type II inhibitor-based **ASDO** kinase system. Despite this variability, we systematically optimized the **ASDO** scaffold to engender a small-molecule inhibitor that displays generality across at least three divergent Ser/Thr kinases bearing a Cys gatekeeper, so far, and **ASDO2** and **ASDO6** display bio-orthogonality versus WT kinases (Figures 1B and 4F). As this system appears to take advantage of not only steric complementarity but also electrostatic interactions, to engender specificity toward Cys-gatekeeper kinases, we hypothesized that it may act independently of the canonical AS kinase system, which is based solely on steric complementarity. This theory was validated *in vitro* and will likely change the landscape of future studies involving signaling pathways in cells and disease models. These multiple AS/**ASDO** kinase systems along with the *Ele-Cys* and ES kinase systems (systems that utilize electrophilic quinazoline and 5'-electrophilic adenosine scaffolds) now provide an ensemble of chemical–genetic tools to explore differential and independent kinase inhibition across at least two kinases in cells.

Lastly, this system exploits binding to and stabilizing the “DFG-out” conformation of kinases, and we demonstrated the tenability of isolating these **ASDO** co-crystal structures using X-ray crystallography. To date, X-ray crystal structures of inactive kinase conformations across the kinome are sparse,^{19,28} but the **ASDO** system could potentially be used to generate X-ray crystal structures of other inactive kinase conformations. This technology, therefore, has great potential to galvanize drug discovery efforts by providing new “DFG-out” X-ray crystal structures that would assist with rational, *in silico* drug design efforts.

■ METHODS

Kinase Assays. Immunoprecipitation and radioactive kinase assays were performed as described previously.²¹ The catalytically dead mutant D174A-GWL was used as a control for inhibition.

Aurora-A and xlCDK1 assays were carried out like FLAG-GWL immunoprecipitation kinase assays were. N-Terminally tagged FLAG-Aurora-A³² kinase and C-terminally tagged MYC-xlCDK1 were overexpressed in HEK 293T cells using the standard phosphate-mediated transfection method. Cdk1 assays were carried out by incubating HEK 293T lysates containing MYC-CDK1 with 4 µg of the anti-c-Myc antibody and immunoprecipitation with 5 µL of Dynabeads Protein G (Thermofisher). To detect phosphorylated histones H1 [CDK1 ([Figure S5A](#))] and H3 [1 µg/20 µL reaction (AAK)], the standard kinase reaction mixture was spiked with 0.075 MBq of [γ -³²P]ATP (PerkinElmer) per 20 µL reaction mixture. After the reaction was stopped with 5 µL of 5X SDS loading buffer and boiled for 5 min at 95 °C, the mixture was resolved via sodium dodecyl sulfate–polyacrylamide gel electrophoresis [4 to 15% Criterion precast gels (Bio-Rad Laboratories) or 13% (v/v) sodium dodecyl sulfate–polyacrylamide gels]. Staining with Coomassie blue revealed ~28 and 21 kDa bands that were imaged by autoradiography. All concentration-dependent kinase assays were performed thrice, and quantitation of activity [phospho-signal(radioactive/densitometry):kinase loading ratio] using ImageJ (version 1.47) of the average normalized percent kinase activity ± the standard deviation was performed using Prism 6.0. Nonlinear regression using Prism 6.0 was used to calculate IC₅₀ values.

Crystallization and Data Collection. Aurora-A (containing mutations L210C, C290A, and C393A)³¹ was co-crystallized with **ASDO2** and **ASDO6** by mixing purified protein (500 µM) with compound (**ASDO2**, 500 µM; **ASDO6**, 1 mM) in a 1:1 protein:ligand ratio, before setting up sitting-drop vapor diffusion experiments at 22 °C, during which 0.25 µL of the complex was mixed with 0.25 µL of the crystallization buffer and equilibrated against a well volume of 50 µL.

Crystals of Aurora-A bound to **ASDO2** were obtained under condition F6 of the PEGs II Suite [0.2 M ammonium sulfate, 0.1 M trisodium citrate (pH 5.6), and 25% (w/v) polyethylene glycol 4000; Qiagen] and bound to **ASDO6** under condition A1 of the JCSG+ Suite [0.2 M lithium sulfate, 0.1 M sodium acetate (pH 4.5), and 50% (w/v) polyethylene glycol 400; Qiagen]. No additional cryoprotectant was added as the crystals were deemed already cryoprotected from their crystallization conditions. The crystals were cryocooled in liquid nitrogen, and no formation of ice was observed. Diffraction data to 2.4 Å (**ASDO2**) and 2.1 Å (**ASDO6**) resolution were collected at the Diamond Light Source (DLS, Didcot, U.K.) on beamline I04.

Phasing, Model Building, and Refinement. All diffraction data were collected at 100 K. Autoprocessed data sets were generated by automatic integration of the data using the software package XDS followed by processing using the Pointless and Scala programs from the CCP4 software suite. Phases were obtained by molecular replacement using Phaser with a high-resolution structure of ADP-bound Aurora-A C290A/C393A (PDB entry 4CEG) used as the search model. An iterative combination of manual building in Coot and refinement with Phenix.refine produced the final model: PDB entries 6HJK (**ASDO2**) and 6HJJ (**ASDO6**). The protein crystallized in space groups P3₂1 (**ASDO2**) and P6₂2 (**ASDO6**), with a single molecule comprising the asymmetric unit. Crystal data and structural refinement data for **ASDO2** and **ASDO6** can be found in Supplemental Tables 1 and 2.

■ ASSOCIATED CONTENT

Supporting Information

The Supporting Information is available free of charge on the ACS Publications website at DOI: [10.1021/acscchembio.8b00592](https://doi.org/10.1021/acscchembio.8b00592).

Supplementary figures, tables, and schemes, supplementary methods, and characterization of synthetic compounds ([PDF](#))

Accession Codes

6HJK, Aurora-A kinase (L210C, C290A, and C393A) co-crystallized with **ASDO2**, and 6HJJ, Aurora-A kinase (L210C, C290A, and C393A) co-crystallized with **ASDO6**.

■ AUTHOR INFORMATION

Corresponding Author

*CORRESPONDING AUTHOR Cory A. Ocasio; tony.ocasio@crick.ac.uk; +44 (0)2037 963780.

ORCID

Cory A. Ocasio: [0000-0002-4957-4131](https://orcid.org/0000-0002-4957-4131)

John Spencer: [0000-0001-5231-8836](https://orcid.org/0000-0001-5231-8836)

Kevan M. Shokat: [0000-0002-6900-8380](https://orcid.org/0000-0002-6900-8380)

Richard Bayliss: [0000-0003-0604-2773](https://orcid.org/0000-0003-0604-2773)

Present Address

#C.A.O.: The Francis Crick Institute, London NW1 1AT, U.K.

Author Contributions

②C.A.O. and A.A.W. are joint first authors.

Funding

This work was funded by the European Community's Seventh Framework Program (FP7/2007-2013) under Grant Agreement PIIF-GA-2011-301062 (C.A.O.), Cancer Research UK Program Award C24461/A23302 (R.B.), and MRC CASE Industrial Studentship MR/K016903 (R.B.).

Notes

The authors declare no competing financial interest.

■ ACKNOWLEDGMENTS

The authors thank H. Hochegger, M. Malumbres, and M. Alvarez-Fernández for donating reagents such as GWL, AAK, and xlCdk1 mammalian expression constructs and primary MEFs containing loxP sites flanking exon 4 of the murine GWL gene. The authors also acknowledge LifeArc (formerly MRC Technology) for contributing funding toward to the Ph.D. position of P. McIntyre, A. Oliver for assisting with *in silico* and bioinformatics approaches for identifying GWL sogg mutations, and S. Ward for granting us access to the synthetic chemistry resources of the Sussex Drug Discovery Center.

■ REFERENCES

- (1) Manning, G., Whyte, D. B., Martinez, R., Hunter, T., and Sudarsanam, S. (2002) The Protein Kinase Complement of the Human Genome. *Science* 298, 1912–1934.
- (2) Elphick, L. M., Lee, S. E., Gouverneur, V., and Mann, D. J. (2007) Using Chemical Genetics and ATP Analogues To Dissect Protein Kinase Function. *ACS Chem. Biol.* 2, 299–314.
- (3) Apsel, B., Blair, J. A., Gonzalez, B., Nazif, T. M., Feldman, M. E., Aizenstein, B., Hoffman, R., Williams, R. L., Shokat, K. M., and Knight, Z. A. (2008) Targeted polypharmacology: discovery of dual inhibitors of tyrosine and phosphoinositide kinases. *Nat. Chem. Biol.* 4, 691–699.
- (4) Barouch-Bentov, R., and Sauer, K. (2011) Mechanisms of drug resistance in kinases. *Expert Opin. Invest. Drugs* 20, 153–208.
- (5) Fedorov, O., Muller, S., and Knapp, S. (2010) The (un)targeted cancer kinome. *Nat. Chem. Biol.* 6, 166–169.
- (6) Bishop, A. C., Ubersax, J. A., Petsch, D. T., Matheos, D. P., Gray, N. S., Blethrow, J., Shimizu, E., Tsien, J. Z., Schultz, P. G., Rose, M. D., Wood, J. L., Morgan, D. O., and Shokat, K. M. (2000) A chemical switch for inhibitor-sensitive alleles of any protein kinase. *Nature* 407, 395–401.
- (7) Lopez, M. S., Choy, J. W., Peters, U., Sos, M. L., Morgan, D. O., and Shokat, K. M. (2013) Staurosporine-derived inhibitors broaden

- the scope of analog-sensitive kinase technology. *J. Am. Chem. Soc.* 135, 18153–18159.
- (8) Zhang, C., Lopez, M. S., Dar, A. C., Ladow, E., Finkbeiner, S., Yun, C. H., Eck, M. J., and Shokat, K. M. (2013) Structure-guided inhibitor design expands the scope of analog-sensitive kinase technology. *ACS Chem. Biol.* 8, 1931–1938.
- (9) Garske, A. L., Peters, U., Cortesi, A. T., Perez, J. L., and Shokat, K. M. (2011) Chemical genetic strategy for targeting protein kinases based on covalent complementarity. *Proc. Natl. Acad. Sci. U. S. A.* 108, 15046–15052.
- (10) Zhang, C., Kenski, D. M., Paulson, J. L., Bonshtien, A., Sessa, G., Cross, J. V., Templeton, D. J., and Shokat, K. M. (2005) A second-site suppressor strategy for chemical genetic analysis of diverse protein kinases. *Nat. Methods* 2, 435–441.
- (11) Bishop, A., Buzko, O., Heyeck-Dumas, S., Jung, I., Kraybill, B., Liu, Y., Shah, K., Ulrich, S., Witucki, L., Yang, F., Zhang, C., and Shokat, K. M. (2000) Unnatural Ligands for Engineered Proteins: New Tools for Chemical Genetics. *Annu. Rev. Biophys. Biomol. Struct.* 29, 577–606.
- (12) Koch, A., Rode, H. B., Richters, A., Rauh, D., and Hauf, S. (2012) A chemical genetic approach for covalent inhibition of analogue-sensitive aurora kinase. *ACS Chem. Biol.* 7, 723–731.
- (13) Kung, A., Schimpl, M., Ekanayake, A., Chen, Y. C., Overman, R., and Zhang, C. (2017) A Chemical-Genetic Approach to Generate Selective Covalent Inhibitors of Protein Kinases. *ACS Chem. Biol.* 12, 1499–1503.
- (14) Kung, A., Chen, Y. C., Schimpl, M., Ni, F., Zhu, J., Turner, M., Molina, H., Overman, R., and Zhang, C. (2016) Development of Specific, Irreversible Inhibitors for a Receptor Tyrosine Kinase EphB3. *J. Am. Chem. Soc.* 138, 10554–10560.
- (15) Blair, J. A., Rauh, D., Kung, C., Yun, C. H., Fan, Q. W., Rode, H., Zhang, C., Eck, M. J., Weiss, W. A., and Shokat, K. M. (2007) Structure-guided development of affinity probes for tyrosine kinases using chemical genetics. *Nat. Chem. Biol.* 3, 229–238.
- (16) Serafimova, I. M., Pufall, M. A., Krishnan, S., Duda, K., Cohen, M. S., Maglathlin, R. L., McFarland, J. M., Miller, R. M., Frodin, M., and Taunton, J. (2012) Reversible targeting of noncatalytic cysteines with chemically tuned electrophiles. *Nat. Chem. Biol.* 8, 471–476.
- (17) Gushwa, N. N., Kang, S., Chen, J., and Taunton, J. (2012) Selective Targeting of Distinct Active Site Nucleophiles by Irreversible Src-Family Kinase Inhibitors. *J. Am. Chem. Soc.* 134, 20214–20217.
- (18) Cohen, M. S., Zhang, C., Shokat, K. M., and Taunton, J. (2005) Structural Bioinformatics-Based Design of Selective, Irreversible Kinase Inhibitors. *Science* 308, 1318–1321.
- (19) Liu, Y., and Gray, N. S. (2006) Rational design of inhibitors that bind to inactive kinase conformations. *Nat. Chem. Biol.* 2, 358–364.
- (20) Mochida, S., Maslen, S. L., Skehel, M., and Hunt, T. (2010) Greatwall phosphorylates an inhibitor of protein phosphatase 2A that is essential for mitosis. *Science* 330, 1670–1673.
- (21) Ocasio, C. A., Rajasekaran, M. B., Walker, S., Le Grand, D., Spencer, J., Pearl, F. M. G., Ward, S. E., Savic, V., Pearl, L. H., Hochegger, H., and Oliver, A. W. (2016) A first generation inhibitor of human Greatwall kinase, enabled by structural and functional characterisation of a minimal kinase domain construct. *Oncotarget* 7, 71182–71197.
- (22) Wang, L., Luong, V. Q., Giannini, P. J., and Peng, A. (2014) Mastl kinase, a promising therapeutic target, promotes cancer recurrence. *Oncotarget* 5, 11479–11489.
- (23) Burgess, A., Vigneron, S., Brioudes, E., Labbe, J. C., Lorca, T., and Castro, A. (2010) Loss of human Greatwall results in G2 arrest and multiple mitotic defects due to deregulation of the cyclin B-Cdc2/PP2A balance. *Proc. Natl. Acad. Sci. U. S. A.* 107, 12564–12569.
- (24) Grant, B. D., Hemmer, W., Tsigelny, I., Adams, J. A., and Taylor, S. S. (1998) Kinetic Analyses of Mutations in the Glycine-Rich Loop of cAMP-Dependent. *Biochemistry* 37, 7708–7715.
- (25) Dar, A. C., Das, T. K., Shokat, K. M., and Cagan, R. L. (2012) Chemical genetic discovery of targets and anti-targets for cancer polypharmacology. *Nature* 486, 80–84.
- (26) Tolstoluzhsky, N., Nikolaienko, P., Gorobets, N., Van der Eycken, E. V., and Kolos, N. (2013) Efficient Synthesis of Uracil-Derived Hexa- and Tetrahydropyrido[2,3-d]pyrimidines. *Eur. J. Org. Chem.* 2013, S364–S369.
- (27) Dar, A. C., and Shokat, K. M. (2011) The evolution of protein kinase inhibitors from antagonists to agonists of cellular signaling. *Annu. Rev. Biochem.* 80, 769–795.
- (28) Hari, S. B., Merritt, E. A., and Maly, D. J. (2013) Sequence determinants of a specific inactive protein kinase conformation. *Chem. Biol.* 20, 806–815.
- (29) Alvarez-Fernandez, M., Sanchez-Martinez, R., Sanz-Castillo, B., Gan, P. P., Sanz-Flores, M., Trakala, M., Ruiz-Torres, M., Lorca, T., Castro, A., and Malumbres, M. (2013) Greatwall is essential to prevent mitotic collapse after nuclear envelope breakdown in mammals. *Proc. Natl. Acad. Sci. U. S. A.* 110, 17374–17379.
- (30) Alexander, L. T., Mobitz, H., Drueckes, P., Savitsky, P., Fedorov, O., Elkins, J. M., Deane, C. M., Cowan-Jacob, S. W., and Knapp, S. (2015) Type II Inhibitors Targeting CDK2. *ACS Chem. Biol.* 10, 2116–2125.
- (31) Burgess, S. G., and Bayliss, R. (2015) The structure of C290A:C393A Aurora A provides structural insights into kinase regulation. *Acta Crystallogr., Sect. F: Struct. Biol. Commun.* 71, 315–319.
- (32) Hegarat, N., Smith, E., Nayak, G., Takeda, S., Eyers, P. A., and Hochegger, H. (2011) Aurora A and Aurora B jointly coordinate chromosome segregation and anaphase microtubule dynamics. *J. Cell Biol.* 195, 1103–1113.